

Ion-impact Excitation for High Precision GCR: Improvements of the Semi-classical, Impact Parameter Approach

Matthew M. Bluteau

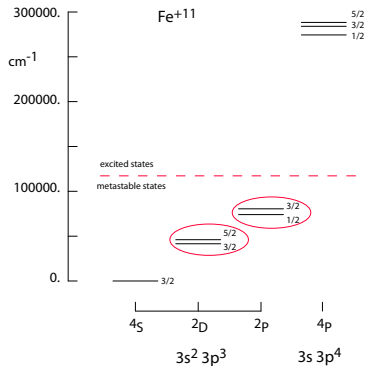
ADAS, University of Strathclyde/CCFE/JET

2 October 2015

INAF — Osservatorio Astrofisico di Catania



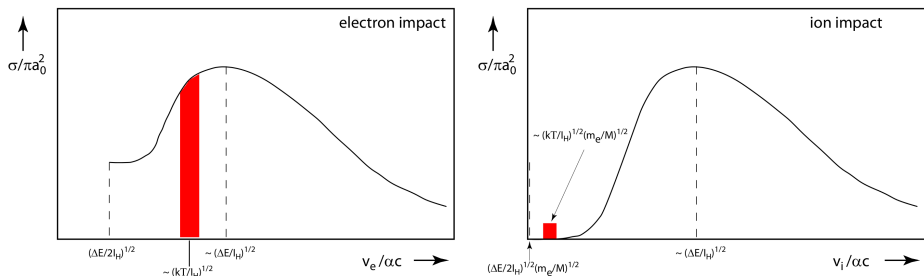
Motivation: Metastable, Fine-structure Transitions



- As previously explained (see GCR presentation by A. Giunta), *ic*-resolved GCR will require rate coefficients for transitions between the fine-structure levels of metastable terms in an ion — e.g. circled levels in figure.
- Necessarily, the transitions will be of the **quadrupole (E2)** type: dipole excitation is excluded by parity conservation within a term.
- The relatively small energy level differences mean ion-impact excitation can become significant — next slide.

Electron-impact vs. Ion-impact

- Discrepancies in the general structure of electron and ion impact cross-sections as well as where the thermal distributions of the colliding species lie explain why ion-impact favours small energy level differences.
- Increased projectile ion speed distributions can also help: at ITER, we will have ion temperatures $T_i \sim 8$ keV, fast fusion alphas $E_{\alpha:D-T} = 3.5$ MeV, and ionised neutral beam atoms $E_{NB} \sim 1$ MeV [1].



Working in atomic units (au), $\Delta E / I_H$ is the transition energy, I_H is the ionization potential of hydrogen in the same units as ΔE , and σ is the cross-section for the arbitrary transition from the target ion level i to j . The temperature, T , of both the colliding ion and electron velocity distributions (red blocks) is assumed to be equal.

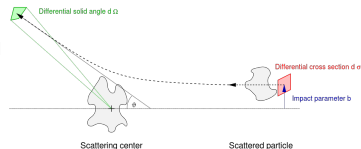
Calculation Technique

- The relatively large mass, m_p , of an ion projectile results in an impractically large number of partial waves in the close-coupling region near the target, meaning a *semi-classical* approach is appropriate versus a fully quantum mechanical one.
- *Coulomb excitation* as per Alder et al [2]: the ion projectile follows a classical trajectory determined by scattering in a Coulomb field, and the excitation probability of the target is obtained through first-order, time dependent perturbation theory.
- The Coulomb excitation differential cross-section is thus given by:

$$d\sigma_{i \rightarrow j} = P_{i \rightarrow j}(\theta) \frac{1}{4\pi} \left(\frac{z_t z_p}{E_p} \right)^2 \csc^4(\theta/2) d\Omega, \quad (1)$$

- $P_{i \rightarrow j}(\theta)$ is the transition probability for a given trajectory, and the remainder of the theory will address its specification.
- z_t , z_p are the target and projectile charges, respectively.
- E_p is the geometric mean of the projectile kinetic energy:

$$E_p = \sqrt{E_{p,i} E_{p,f}}$$
- θ is the scattering angle in the cms frame.
- The boxed term is the classical Rutherford differential cross-section.



[https://commons.wikimedia.org/w/index.php?title=File:](https://commons.wikimedia.org/w/index.php?title=File:Differential_cross_section.svg&oldid=138819349)

[Differential_cross_section.svg&oldid=138819349](https://commons.wikimedia.org/w/index.php?title=File:Differential_cross_section.svg&oldid=138819349)

The Transition Probability, $P_{i \rightarrow j}$

- First-order, time-dependent perturbation theory tells us:

$$P_{i \rightarrow j} = \frac{1}{\omega_i} \sum_{M_i M_j} |b_{ij}(t = \infty)|^2; \quad b_{ij} = \frac{1}{i\hbar} \int_{-\infty}^{\infty} \langle j | H(t) | i \rangle e^{i\omega t} dt. \quad (2)$$

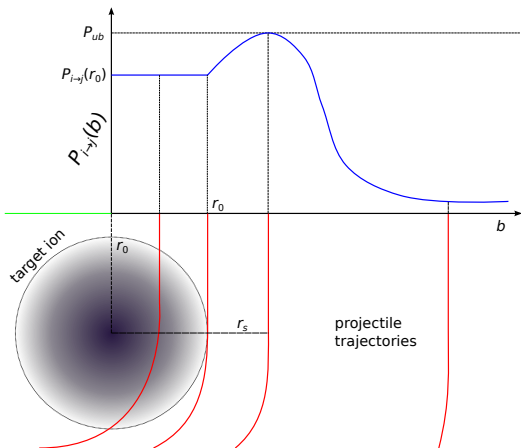
- After a great deal of algebra and the use of $\frac{1}{|r_p - r|} \approx \sum_{\lambda} P_{\lambda}(\hat{r}_p \cdot \hat{r}) r^{\lambda} / r_p^{\lambda+1}$, we find for the quadrupole case:

$$P_{i \rightarrow j}(E2) = 4m_0 B(E2) z_p^{-2} z_t^{-4} E_{p,i} E_p^2 \sin^4(\theta/2) \frac{df_{E2}}{d\Omega}(\theta, \xi), \quad (3)$$

where $B(E2)$ is the reduced, quadrupole atomic transition probability that we obtain from our atomic structure calculations, m_0 is the reduced mass of the projectile and target, and ξ is the dimensionless, symmetrized adiabaticity parameter: $\xi \propto E_p^{-3/2}$.

- $\frac{df_{E2}}{d\Omega}(\theta, \xi)$ is the differential excitation cross-section function made up of classical orbital integrals that fall out of the right hand equation in 2; these integrals need to be computed numerically, and a table of pre-computed values due to Alder et al [2] has been employed in numerous computer programs — an area for improvement.

Detailed Considerations and History of $P_{i \rightarrow j}$



- Coulomb excitation calculations have a long history, but the subject must be revisited because numerous mistakes have been made when calculating $P_{i \rightarrow j}$.
- Penetrating collisions and the strong-coupling region need to be treated correctly, as in the figure.
- Codes due to Bely and Faucher [3] and Bahcall and Wolf [4] both treat penetrating collisions incorrectly, leading to the incorrect high energy scaling of the cross-section.
- Seaton [5] gets this right but does not ensure the correct fall-off of the cross-section.
- Burgess and Tully [6] summarize the mistakes and present a completely corrected form of the theory, but their resulting code has been lost.

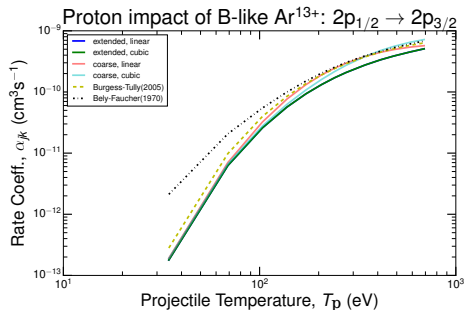
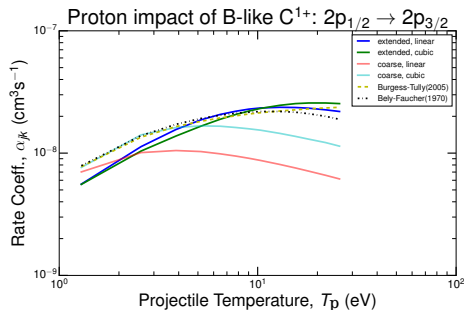
Objectives

End Goal

Replace the lost Burgess and Tully [6] semi-classical Coulomb excitation code with our own code that will assimilate fully within the ADAS framework.

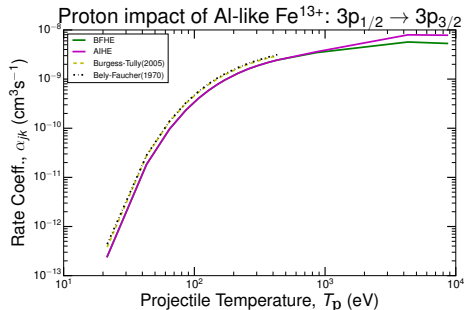
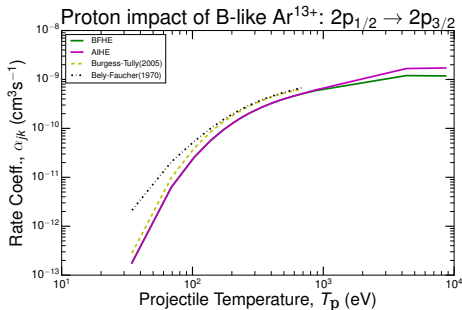
- First step: use the proton-impact Bely-Faucher [3] codes as source of initial ion-impact data and make necessary minor modifications as a learning experience and in an effort to mitigate flaws.
- Completed modifications:
 - Generalization to permit any bare nucleus projectile (ie m_p and z_p parameters introduced)
 - Extension of $\frac{df_{E2}}{d\Omega}(\theta, \xi)$ data table: higher mesh density and lower values of ξ (higher E_p values for cross-sections) — more on next slide
 - Incorporation of Bethe limit, Ω_{lim} , from structure calculation for extrapolation of collision data during rate coefficient calculation — two slides forward

Extension of $\frac{df_{E2}}{d\Omega}(\theta, \xi)$ Data Table



- 'extended' refers to the use of the extended $\frac{df_{E2}}{d\Omega}(\theta, \xi)$ data table, and 'coarse' to the original, limited data table from Alder et al.
- 'linear' refers to linear interpolation of the cross-sections between the values obtained using the $\frac{df_{E2}}{d\Omega}(\theta, \xi)$ table, and 'cubic' refers to cubic spline interpolation
- In theory, the Bely-Faucher (1970) results should lie on top of our coarse, linear results as these codes should be nearly identical; however, provenance is uncertain

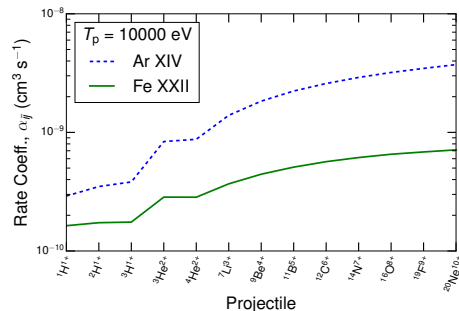
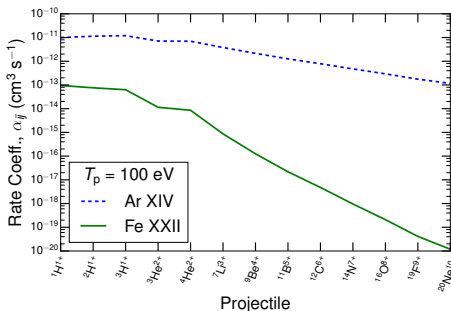
Inclusion of Ω_{lim} for Rate Coefficient Calculation



- BFHE = original Bely-Faucher strategy for high energy contribution of cross-section to rate coefficient: $\sigma_{ij}(E_f) \cdot E_f = \text{cons.} = C$ and so $\alpha^{\text{HE}} = C \int e^{-E_i/kT} d(E_i/kT) = C$
- AIHE = fit a line to last *collision strength* and Ω_{lim} and compute improper integrals using analytic form similar to above
- 'Recommended' is extended, cubic, BFHE: use of our extended $\frac{df_{E2}}{d\Omega}(\theta, \xi)$ data table, cubic spline interpolation of cross-sections during integration, and the BFHE scheme

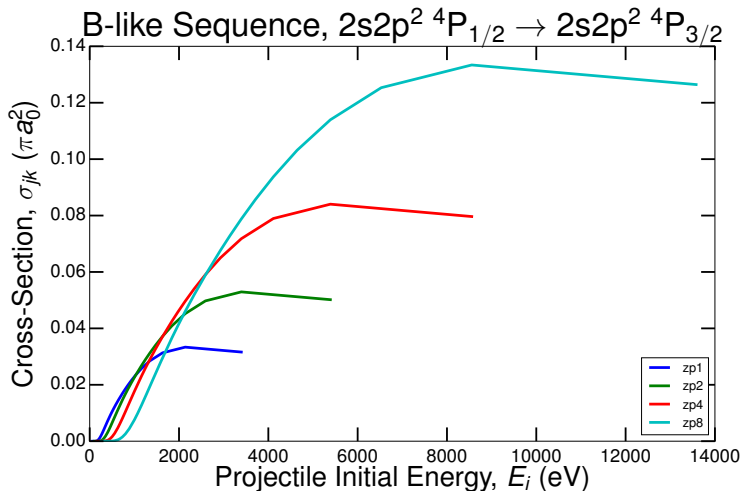
Projectile Variation

B-like Isoseq: $2s2p^2 \ ^4P_{1/2} \rightarrow 2s2p^2 \ ^4P_{3/2}$



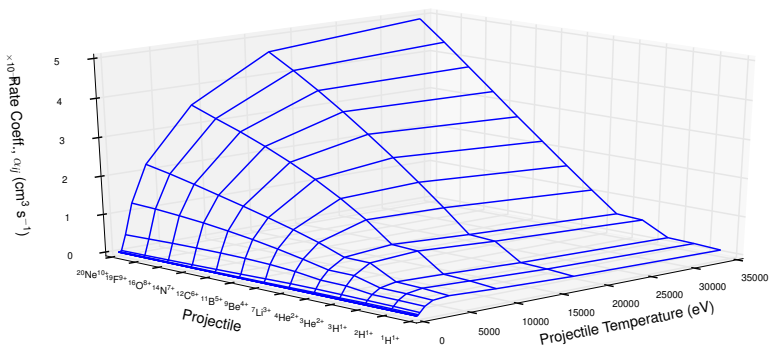
- Change from decreasing function along projectile sequence at lower T_p to increasing function along projectile sequence at higher T_p can be explained by z_p scaling of cross-sections

z_p Variation of Cross-section



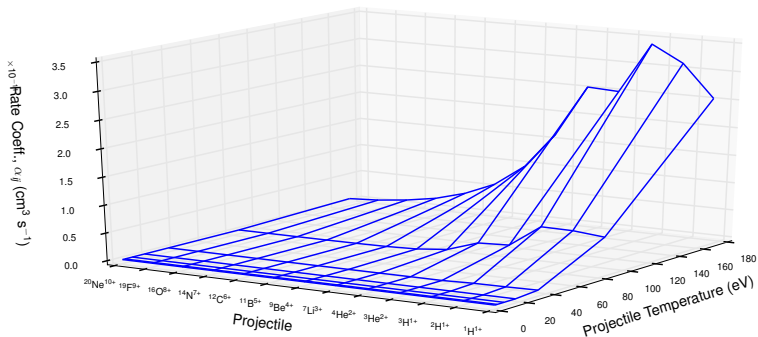
Projectile Variation: 3D High T

B-like Isoseq: $2s2p^2 \ ^4P_{1/2} \rightarrow 2s2p^2 \ ^4P_{3/2}$



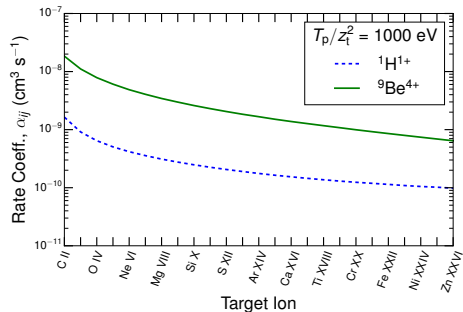
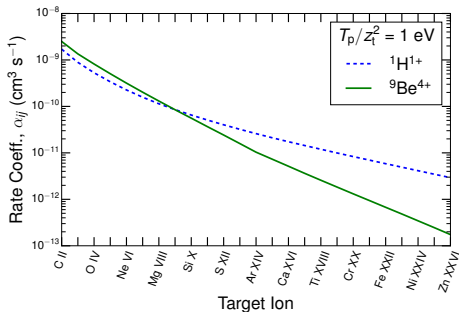
Projectile Variation: 3D Low T

B-like Isoseq: $2s2p^2 \ ^4P_{1/2} \rightarrow 2s2p^2 \ ^4P_{3/2}$



Target Variation

B-like Isoseq: $2s2p^2 \ ^4P_{1/2} \rightarrow 2s2p^2 \ ^4P_{3/2}$



- Decreasing $\alpha_{i \rightarrow j}$ along target sequence at lower T_p is likely again due to repulsive effect at threshold.

Concluding Remarks

- We have successfully implemented a set of codes which can calculate ion-impact excitation cross-sections and rate coefficients using the Coulomb excitation approximation.
- Accommodation of any bare nucleus projectile has been achieved, with correct scaling of rate coefficients and cross-sections achieved
- Expansion of the $\frac{df_{E2}}{d\Omega}(\theta, \xi)$ data table and incorporation of the Bethe limit for collision strength extrapolation have implemented as improvements upon the Bely-Faucher and in preparation of what will be need to be done with our own re-write.
- Preliminary Generalized Collisional-Radiative (GCR) modelling has shown that ion-impact excitation will indeed have an effect upon metastable populations relevant for spectroscopic modelling.
- The next step will be to implement the full prescription of Burgess and Tully in our own code, correctly dealing with penetrating collisions and ensuring the proper high energy behaviour.

References I

- [1] R. Aymar, P. Barabaschi, and Y. Shimomura. The iter design. *Plasma Phys. Control. Fusion*, 44(5):519–565, 2002.
- [2] K. Alder, A. Bohr, T. Huus, B. Mottelson, and A. Winther. Study of nuclear structure by electromagnetic excitation with accelerated ions. *Rev. Mod. Phys.*, 28(4):432–542, October 1956.
- [3] O. Bely and P. Faucher. Fine structure proton excitation rates for positive ions in the $2p$, $2p^5$, $3p$, $3p^6$ series. *Astron. Astrophys.*, 6:88–92, 1970.
- [4] J. Bahcall and R. Wolf. Fine-structure transitions. *Astrophys. J.*, 152:701–729, 1968.
- [5] M. J. Seaton. Excitation of coronal lines by proton impact. *Astrophys. J.*, 127:191–194, 1964.
- [6] A. Burgess and J. A. Tully. On proton excitation of forbidden lines in positive ions. *J. Phys. B: At. Mol. Opt. Phys.*, 38:2629–2644, 2005.